Figure S1

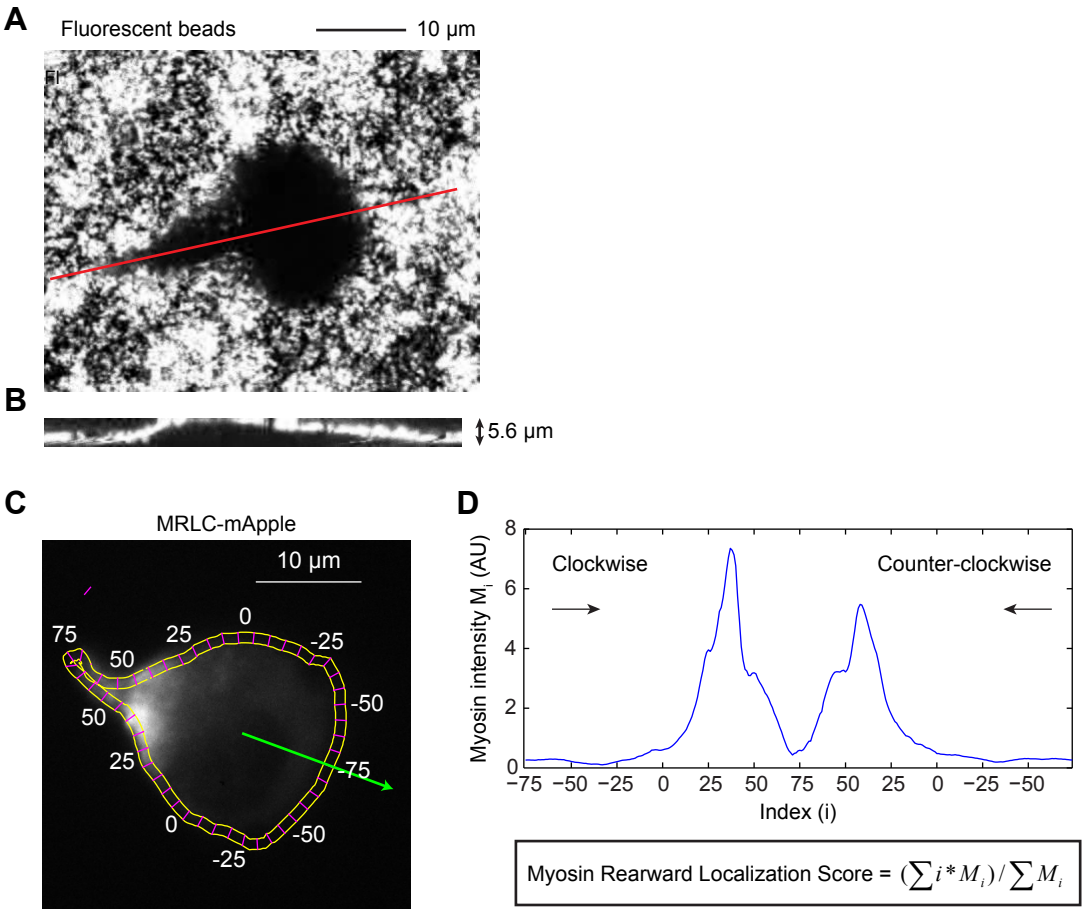
A
Fluorescent beads
10 μm
B
5.6 μm
C
MRLC-mApple
10 μm
75
50
25
0
-25
-50
-75
D
Clockwise
Counter-clockwise
Myosin intensity M_i (AU)
Index (i)
Myosin Rearward Localization Score = $(\sum i * M_i) / \sum M_i$
E
Correlation between protrusion speed (PS) and MRS
PS precedes MRS
MRS precedes PS
Not significant
Time offset (sec)
F
Correlation between protrusion speed (PS) and RRS
PS precedes RRS
RRS precedes PS
Pearson's Correlation
Not significant
Time offset (sec)

Figure S2

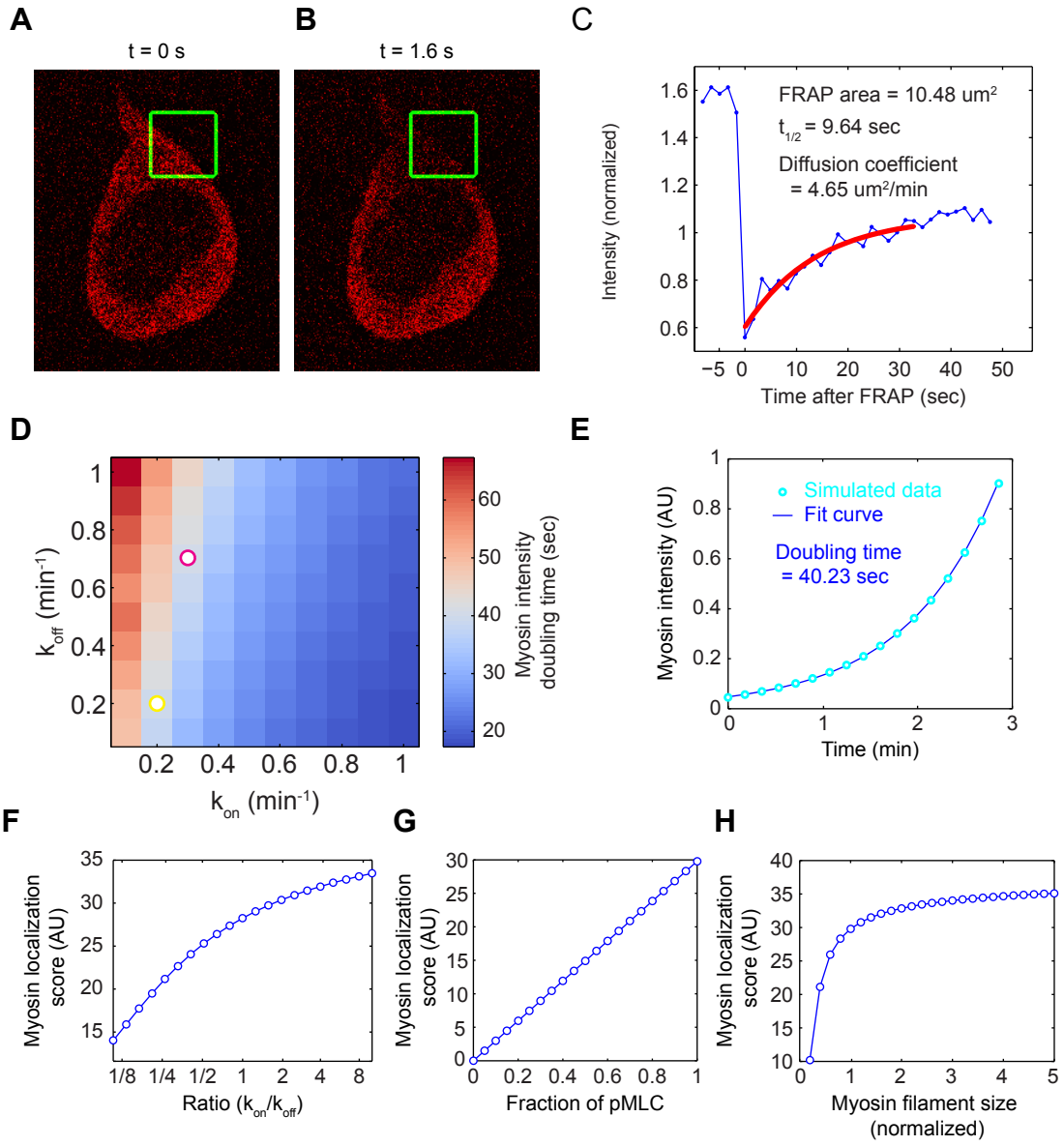
A
t = 0 s
B
t = 1.6 s
C
FRAP area = 10.48 um²
t1/2 = 9.64 sec
Diffusion coefficient
= 4.65 um²/min
Intensity (normalized)
Time after FRAP (sec)
D
koff (min-1)
kon (min-1)
Myosin intensity
doubling time (sec)
E
Simulated data
Fit curve
Doubling time
= 40.23 sec
Myosin intensity (AU)
Time (min)
F
Myosin localization
score (AU)
Ratio (kon/koff)
G
Myosin localization
score (AU)
Fraction of pMLC
H
Myosin localization
score (AU)
Myosin filament size
(normalized)

Figure S3

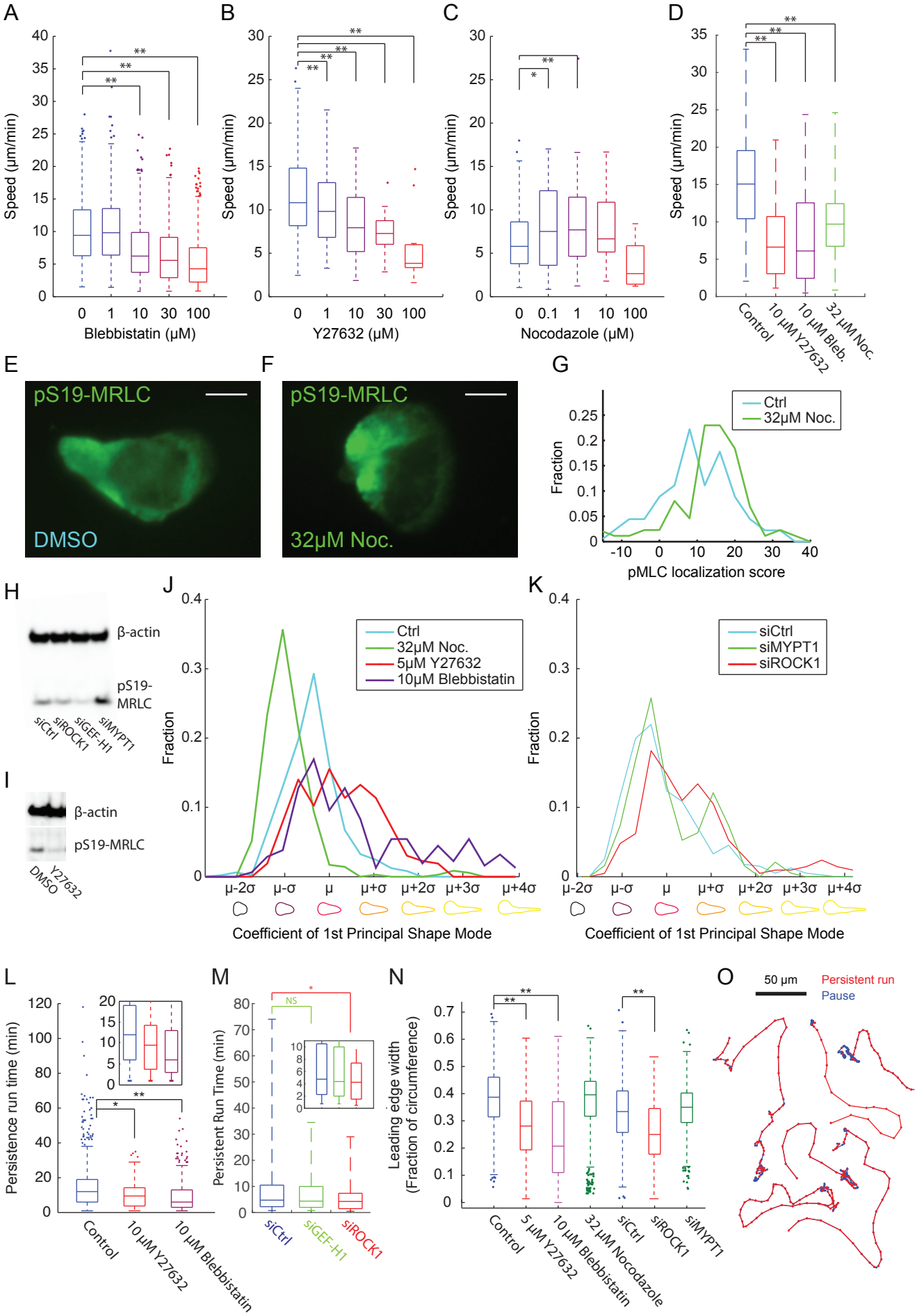
A
B
C
D
Speed (μm/min)
Blebbistatin (μM)
Y27632 (μM)
Nocodazole (μM)
Control
10 μM Y27632
10 μM Bleb.
32 μM Noc.
E
F
G
pS19-MRLC
DMSO
32μM Noc.
Ctrl
32μM Noc.
Fraction
pMLC localization score
H
I
β-actin
pS19-MRLC
siCtrl
siROCK1
siGEF-H1
siMYPT1
DMSO
Y27632
J
K
Ctrl
32μM Noc.
5μM Y27632
10μM Blebbistatin
siCtrl
siMYPT1
siROCK1
Fraction
Coefficient of 1st Principal Shape Mode
L
M
N
O
Persistence run time (min)
Persistent Run Time (min)
Leading edge width (Fraction of circumference)
NS
10 μM Blebbistatin
5 μM Y27632
32 μM Nocodazole
50 μm
Persistent run
Pause

Figure S4

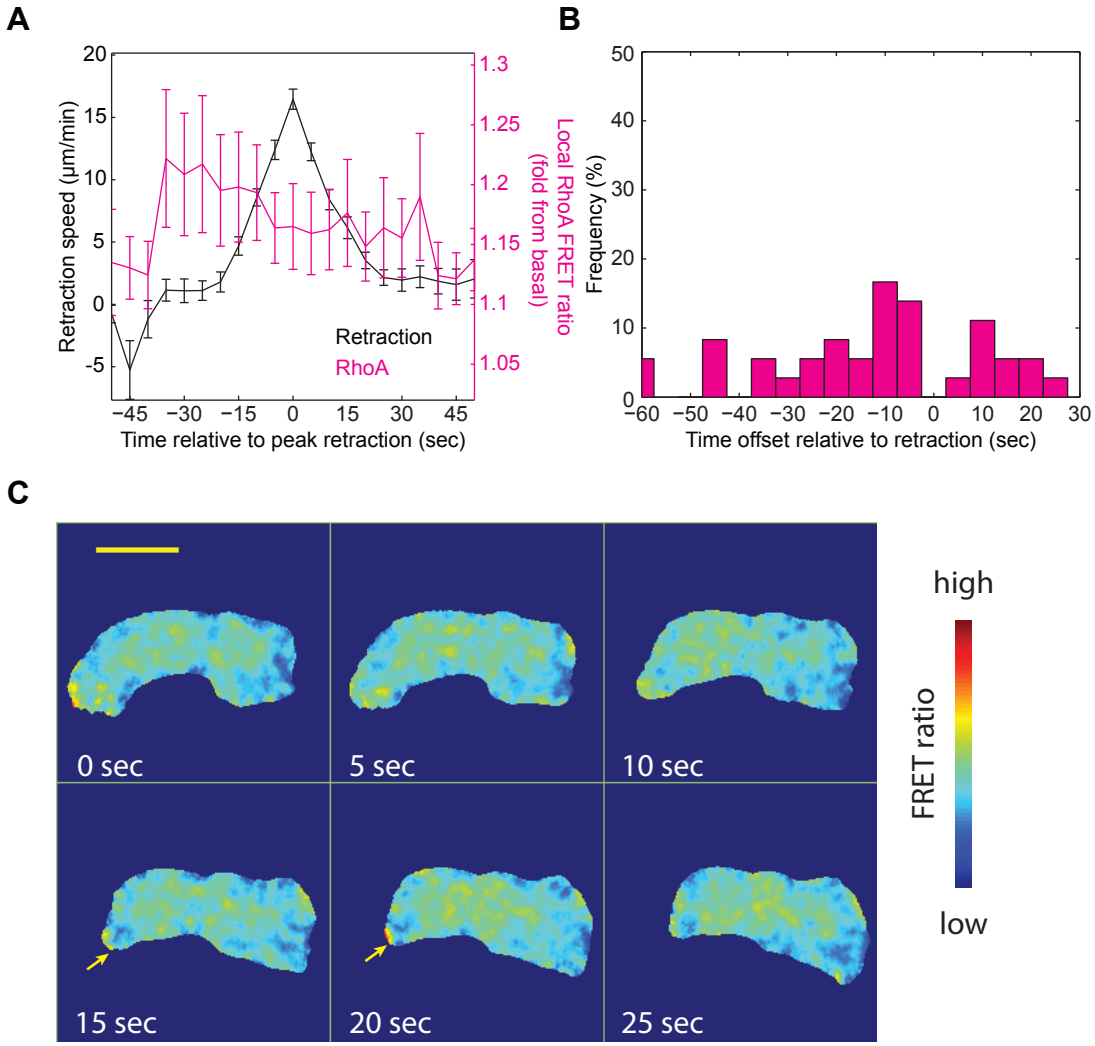
A
B
C
Retraction speed (μm/min)
Local RhoA FRET ratio (fold from basal)
Retraction
RhoA
Time relative to peak retraction (sec)
Frequency (%)
Time offset relative to retraction (sec)
0 sec
5 sec
10 sec
15 sec
20 sec
25 sec
high
FRET ratio
low

Figure S5

A

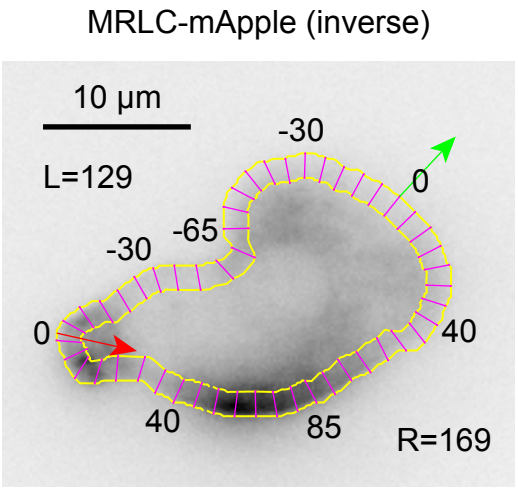

B

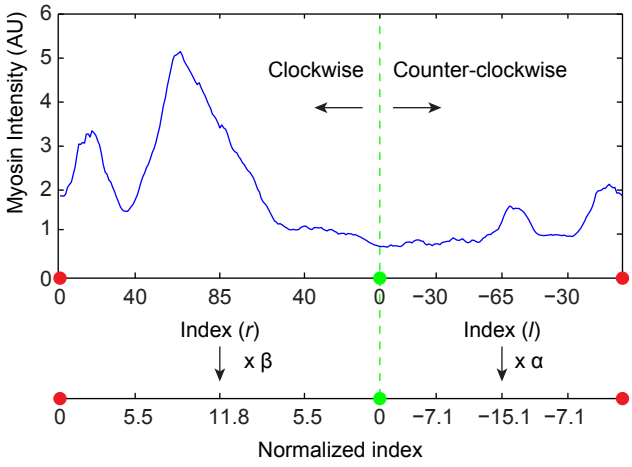

Myosin Left-Right Asymmetry Score =

$$(\alpha\sum l * M_l + \beta\sum r * M_r)/(\sum M_l + \sum M_r)$$

Supplementary figures S1 - S5:

Figure S1. Confinement of migrating HL-60 cells in an under-agarose assay, and calculation of the myosin rearward localization score (MRS) and the RhoA rearward localization score (RRS); related to Figure 1.

(A) The surface of the agarose is coated with Alexa Fluor 568-conjugated beads to visualize the interface between the agarose and the cell. The dark outline of a single cell shows the displacement of the coated agarose pad.

(B) A *z*-stack of an HL60 cell reconstructed from 28 slices with confocal microscopy. The horizontal direction is along the red line shown in (A). The profile of the fluorescent beads shows the height of the cell from the front to the rear, and confirms that the cells are indeed migrating in confinement.

(C) A fluorescent image of a migrating HL60 expressing MRLC-mApple. The green arrow starts from the cell centroid, and points towards the direction of cell centroid movement. This direction is used to define the indices around the cell contour, from -75 to 75 and back to -75. The two yellow contours are 1 μm apart, and the magenta lines are 6 grid points apart (2% of the total circumference, and about 0.9 μm). The boxes between the yellow lines and the magenta lines represent the region used to calculate the average myosin intensity.

(D) Local myosin intensity around the cell contour, plotted against the indices. The myosin rearward localization score was calculated by the formula shown in the black box. i represents the index at each point along the cell boundary, and M_i represents the corresponding myosin intensity at index i.

(E) Cross-correlation between the protrusion speed (PS) and the myosin rearward localization score (MRS). A negative offset means the protrusion precedes the MRS. To sum up all the results, we concatenated the traces of PS and MRS from all movies (6 different cells, 73 minutes of movies and 1490 time points). The thick black line represents the cross-correlation curve of the concatenated traces. The magenta shaded region represents a correlation that is below 95% confidence interval, obtained by bootstrapping. The thin lines at the background represent the cross-correlation curve of individual cells.

(F) Cross-correlation between the protrusion speed (PS) and the RhoA rearward localization score (RRS). RRS is calculated the same way as MRS shown in (a-b), except that the fluorescent intensity of myosin is replaced by RhoA FRET ratio. A negative offset means the protrusion precedes the RRS. To sum up all the results, we concatenated

the traces of PS and RRS from all movies (15 different cells, 88 minutes of movies and 1056 time points). The thick black line represents the cross-correlation curve of the concatenated traces. The magenta shaded region represents a correlation that is below 95% confidence interval, obtained by bootstrapping. The thin lines in the background represent the cross-correlation curve of individual cells.

Figure S2. A simple mathematical model that recapitulates several aspects of myosin dynamics; related to Figure 2.

(A-C) We performed fluorescence recovery after photobleaching (FRAP) experiments on HL60 cells treated with 5 μM Y27632, and recorded the recovery dynamics to estimate the diffusion coefficient of cytoplasmic myosin. Images are shown immediately before (A) and 1.6 sec after (B) photobleaching. (C) A representative recovery curve from a FRAP experiment, showing the intensity over time for the region denoted by the green box in (A) and (B). The red line shows the best exponential fit to the indicated region of the recovery curve.

(D) We simulated the myosin dynamics using different combinations of k_{on} and k_{off} values. The resulting doubling time of myosin intensity was shown in the heat map. The magenta and the yellow circles represented two paramter sets that are closest to our experimental measurement of myosin doubling time. We chose k_{on} =0.3 min^{-1} and k_{off} =0.7 min^{-1} for our simulation in Figures 2I, 2J, and S2F.

(E) The simulated accumulation of myosin intensity can be well-fit by a single exponential curve.

(F) Expected changes in myosin localization score as a function of the ratio between k_{on} and k_{off}.

(G) Expected changes in myosin localization score as a function of the phosphorylation of the MRLC.

(H) Expected changes in myosin localization score as a function of the size of myosin filaments.

Figure S3. Comparison between MRLC-mApple and pSer19-MRLC immunofluorescence, and the effect of cell shape and migration persistence under various drug and siRNA perturbations; related to Figure 3

(A-D) Cell speed decreases with increasing concentration of (A) blebbistatin, (B) Y27632, and (C) nocodazole. The data were used to identify proper concentrations of chemical inhibitors in our experiments, summarized in (D).

(E-F)Representative snapshots of (E) DMSO-treated (control) or (F) nocodazole-treated HL60 cells immunolabeled with antibody targeting pS19-MRLC. Scale bars are 10 μm.

(G) Histogram of pMLC rearward localization score under DMSO (1317 cells) and nocodazole treatment (578 cells), showing consistency with MRLC-mApple results in Figures 3E and 3F. The pMLC rearward localization score is calculated the same way as MRS in Figure S1C-S1D, except the immunofluorescence intensity of pMLC antibody is used instead of MRLC-mApple fluorescent intensity.

(H) Western blot of HL60 lysate after siRNA knockdown of ROCK1, GEF-H1 and MYPT1, showing the change of pS19-MRLC level. Western blot of β-actin antibody serves as loading control.

(I) Western blot of HL60 lysate after Y27632 treatment, showing the reduction of pS19-MRLC level. Western blot of β-actin antibody serves as loading control.

(J) Chemical inhibitors of myosin dynamics also change cell shape. To quantify cell shape, we established a library of 137 unperturbed cells and 822 different cell shapes. We performed principal component analysis on this cell shape library to identify the major modes of shape variations. The first principal mode of variation corresponds to the length of the cell. We projected all the cell shapes under different perturbations to this first principal mode, and obtained a coefficient for each cell shape. This coefficient could be considered as a metric for the length of the cell. Using this metric, we show distribution of cell length under 4 different drug conditions: DMSO (N=492), 32 μM nocodazole (N=351), 5μM Y27632 (N=264), and 10μM blebbistatin (N=313). Myosin inhibitors Y27632 and blebbistatin make cells longer, while nocodazole makes cells rounder.

(K) siRNA perturbation of myosin dynamics and the effect of cell shape. The length of cell is quantified as described in (H). siRNA knockdown of ROCK1 result in longer cells, while the change of cell shape in MYPT1 knockdown cells are not significantly different from control. siCtrl (N=396), siROCK1 (N=209), siMYPT1 (N=190).

(L) Box plot of the persistence run time. Inset is a magnified version of the region of the plot corresponding to run times <10 min to highlight the average and the 25% and 75% of each distribution. Cell numbers: control (1066 cells), Y27632 (45 cells), blebbistatin (682 cells).

(M) Box plot of the persistence run time. Inset is a magnified version of the region of the plot corresponding to run times <20 min to highlight the average and the 25% and 75%

of each distribution. Cell numbers: siCtrl (218 cells), siGEF-H1 (132 cells), siROCK1 (242 cells).

(N) Box plot of the width of leading edge, as normalized by the circumference. Control (585 shapes from 117 cells), Y27632 (220 shapes from 44 cells), blebbistatin (324 shapes from 65 cells), nocodazole (680 shapes from 136 cells), siCtrl (726 shapes from 66 cells), siROCK1 (649 shapes from 59 cells), siMYPT1 (737 shapes from 67 cells).

For (A-D) and (L-N), * represents significant differences with $p < 0.05$, ** represents significant differences with $p < 0.005$. The p values were obtained using Student's t-test.

(O) 6 single-cell trajectories are shown to demonstrate the selection of the speed threshold in our analysis for persistent run time. The positions of the cells were recorded every minute. A displacement greater than 2.1 μm/min is colored red, representing a persistent moving phase. A displacement lower than 2.1 μm/min is colored blue, representing a pausing phase.

Figure S4. Correlation between RhoA activity and edge retraction velocity with highly variable temporal offset; related to Figure 4.

(A) Average dynamics of the RhoA activity (Data averaged from 37 flashes from 13 cells) and the local edge retraction speed. The temporal traces of the two values are registered to the peak of the retraction speed (defined as time 0). Error bar represents the standard error of the mean.

(B) Distribution of temporal offset between local RhoA FRET ratio and local retraction velocity (N=37), showing a highly variable temporal offset. A positive value means RhoA dynamics lags behind retraction velocity.

(C) A montage of an example movie of RhoA FRET sensor expressing cell during a retraction event. 0 second marks the beginning of a retraction. The RhoA FRET ratio fluctuates at the retracting edge. In this example, RhoA activity reaches the peak at 20 seconds after the onset of retraction, as indicated by the yellow arrows. Scale bar is 10 μm.

Figure S5. Calculation of the myosin left-right asymmetry score; related to Figure 5.

(A) An inverted image of a turning HL60 cell expressing MRLC-mApple. The green arrow represents the protrusion direction (as defined in the Methods section) and the red arrow represents the direction of uropod movement. Similar to Fig. S2a, the two yellow

contours are 1 μm apart, and the magenta lines are 6 grid points apart (2% of the total circumference, and about 0.9 μm). The boxes between the yellow lines and the magenta lines represent the region used to calculate the average myosin intensity.

(B) Local myosin intensity around the cell contour, plotted against the indices. The myosin left-right asymmetry score was calculated by the formula shown in the black box. l and r represents the index at each point along the cell boundary. M_l and M_r represents the corresponding myosin intensity at index l or r. α and β were the scalar used to normalize the indices, in order to compensate for the uneven number of grid points in the left and right side of the cell.

Supplementary movies S1 - S9:

Movie S1: Obtaining protrusion and retraction speeds from cell contours, and calculation of myosin rearward localization score; related to Figure 1. The movie is an illustration of our image analysis procedure. The contour of the cell in each frame was segmented carefully, and contours from consecutive frames were used to obtain the protrusion and retraction speeds.

The myosin rearward localization score (MRS) was used to quantify the localization of myosin at each frame. An MRS of 0 represents uniformly distributed myosin, and a greater value of MRS represents more extreme localization of myosin to the rear. Scale bar = 10μm.

Movie S2: Total internal reflection microscopy (TIRF) of an HL60 cell expressing actin-YFP and MRLC-mApple, shown in the laboratory and cell frame of reference; related to Figure 2. The two lower panels of the movie are registered to the cell frame of reference to emphasize the retrograde flow of fluorescent actin and myosin puncta. Scale bar = 10μm.

Movie S3: Photo-inactivation of blebbistatin by blue light; related to Figure 3. Photo-inactivation of blebbistatin leads to a transient increase of retraction speed, and also results in an increase of protrusion speed and broadening of the lamellipodium. Scale bar = 10μm.

Movie S4: A HL60 cell expressing MRLC-mApple exhibits myosin flashes that are correlated with cell turning; related to Figure 4. Scale bar = 10μm.

Movie S5: An illustration of quantitative analysis on turning HL60 cells; related to Figure 5. The green vector represents the direction of maximal protrusion speed, and the red vector represents the direction of the uropod. The difference of the two directions was defined as the turning angle. The turning angle can be compared with the myosin left-right asymmetry score. Scale bar = 10μm.

Movie S6: TIRF movie of myosin flow in a turning neutrophil expressing MRLC-mApple; related to Figure 5. The movie shows asymmetric myosin retrograde flow closely follows asymmetric protrusion and re-orients the uropod. The images are registered to the cell frame of reference to allow visualization of myosin retrograde flow. Green lines represent the direction of protrusion. Magenta lines represent the direction of the uropod. Blue lines outline the cell contour. Movement of individual myosin puncta in the cell frame of reference were shown for 5 consecutive frames and marked with different colors. The red dots mark the myosin puncta at the current frame, and the green dots mark the myosin puncta 12 seconds before the current frame. Scale bar = 10μm.

Movie S7: A HL60 cell expressing Actin-YFP and MRLC-mApple migrating in a microfluidic channel with right-angle turns; related to Figure 6. From right: overlay, phase-contrast, actin (green), myosin II (red), cell outline (blue) with direction of maximal protrusion (green line).

Movie S8: Migration of chemotactic HL60 cells toward the pathogenic yeast *Candida albicans*; related to Figure 6. Two time-lapse sequences are included. The first shows an untreated cell expressing MRLC-mApple, and the second shows a cell treated with nocodazole. Scale bar = 10μm.

Movie S9: Neutrophil expressing MRLC-GFP migrating in a 3dpf zebrafish embryo; related to Figure 7. Maximal intensity projection along the z-direction was performed on the original 3D confocal z-stacks to obtain this 2D movie. Scale bar = 10μm.